Secondary Flow Injection in Convergent-Divergent Nozzles for Fluidic Thrust Vectoring: A Review

Deepak Gupta[1*]

[1] *Assistant Professor, Department of Aerospace Engineering, GNA University, Phagwara, 144401*

[*] *Corresponding author: deepakgupta7060@gmail.com*

Thrust vectoring using fluidics has been attracting considerable interest as an efficient way to achieve compactness and agility compared to classical mechanical control of the nozzle in contemporary propulsion systems in aviation. In particular, among different possible strategies for thrust vectoring, secondary flow injection into the converging-diverging nozzles seems to be a potential way to control thrust vector via flow manipulation inside the nozzle instead of its mechanical displacement. This paper is a review of flow processes, design parameters, and performance of fluidic thrust vectoring using secondary flow injection in converging-diverging nozzles. It aims to outline the effects of nozzle pressure ratio, secondary/primary pressure ratio, mass flow ratio, position of the injectors, injection angle, and geometry of nozzles on shock formation, boundary layer separation, pressure field variation, and efficiency of vectoring. Main findings regarding the developments in dual-throat, bypass, serpentine, dual-bell, and reacting injection concepts will be reviewed, highlighting trends reported in recent literature. It has been demonstrated that effective thrust vectoring requires an optimal compromise between vectoring capability, thrust loss, and flow stability, where geometrical factors and fluidic control are considered to be design factors of coupled nature. Lastly, the article highlights some of the important areas requiring research, including the development of performance criteria, parametric studies, and experimental validation of data in the case of supersonic and real fluid flows. This review serves as a comprehensive guide for secondary injection in convergent-divergent nozzles.

Keywords: Fluidic Thrust Vectoring, CD Nozzle, Secondary Flow Injection, CFD

Introduction

Due to the need for increased agility and fast response coupled with efficient and small size propulsions, thrust vectoring has become a key technological component in contemporary aerospace vehicles. In the cases of both rocket and air-breathing propulsion, the capability of directing the thrust vectoring without using bulky mechanical components is beneficial due to its reduced weight and simplicity as well as improved reliability and fast response time. Traditional mechanical devices for vectoring the thrust, including gimbal-mounted nozzles, jet vanes, flaps, and plugs, are efficient vectoring devices, although their use involves some drawbacks in the form of added mass, complexity, and thermal loading. Fluidic thrust vectoring is one solution that can solve such problems by utilizing the effects of flow interaction. Secondary flow injection in converging-diverging nozzles is one approach that has been considered continuously

because of its capability of influencing the internal pressure distribution and directing the jet utilizing compressible flow principles[1], [2], [3], [4], [5] [6][7].

The secondary injection in C-D nozzles, in essence, is an approach to flow control based on injecting a secondary flow into the main flow stream at some specific location, angle, and mass flow rate. The injection of the secondary flow interacts with the high-velocity main flow and generates a series of complicated flow patterns, such as oblique shocks, separation of the boundary layer, recirculation zone, reattachment area, and unbalanced pressure distribution on the walls of the nozzle. In this way, the pressure distribution on the walls of the nozzle becomes altered, giving rise to a lateral force and hence deviating the total thrust vector. This kind of control action is not just the result of momentum addition through secondary injection, but is rather caused by the nonlinear interaction between shock wave structure, separation and pressure distribution in the nozzle. Due to the highly nonlinear interactions between all these variables, it is difficult to quantify the performance of secondary injection in terms of a single parameter[8][9].

One of the reasons behind the increasing popularity of the secondary injection technology for thrust vectoring is the ability of this approach to address the needs of the aerospace industry. The rocket nozzles and propulsion systems work under extreme thermal, mechanical, and pressure loads, and it can be challenging to employ conventional moving components in such systems. In such situations, the secondary injection represents a compact and, possibly, reliable means of control for the missiles, launchers, and other advanced propulsion systems. With the secondary injection approach, it is possible to provide thrust vectoring without any mechanical components in the hot exhaust stream and with the application in the fixed nozzles. However, on the other hand, the use of this technology brings certain challenges, such as the loss of the thrust, decreased discharge coefficient, and flow instability under unfavorable injection conditions [10].

The physics of the secondary injection process in a converging-diverging nozzle is highly non-linear and is dependent on many nondimensional numbers. These include nozzle pressure ratio, secondary pressure ratio, secondary-to-primary mass-flow ratio, injector location, injector angle, and geometry of the expansion region of the nozzle. Nozzle pressure ratio characterizes the operating condition of the nozzle and controls the separation or attached nature of the flow and even the shock structure if applicable. Secondary pressure ratio and mass-flow ratio control the intensity of the jet being introduced into the primary flow and hence control pressure distortion and jet penetration. The position of the injector can be particularly important since the Mach number, static pressure, and boundary layer thickness will vary at different stations along the length of the nozzle. Injection in a high Mach number and low static pressure region will result in greater pressure asymmetry and vectoring action, while injection at the exit region may not provide a good vectoring action. Injector Angle also affects the penetration and direction of the secondary flow stream, although in most cases its importance is secondary to the location and pressure of the streams. Moreover, thermodynamic parameters of the injecting fluid, such as the molecular weight, temperature, and compressibility, may affect the mixing process[11][12].

It has been recently proved that geometry and operating condition are not independent variables but are related to each other. For shock vector control serpentine nozzles, it is found out that the secondary and auxiliary injection system can cause a great deal of changes to the region of separation and shock structure, resulting in better thrust-vectoring performance. For bypass dual-throat nozzles, it is revealed that the bypass channel geometry, valve positioning and valve opening direction can greatly influence the internal flow field and vector angle at the end. For the axisymmetric divergent bypass dual-throat systems, it is noted that the bypass flow can contribute to the thrust-vectoring performance without any secondary mass flow and the performance of such configuration will depend on the expansion ratio, throat rounding and bypass width[13].

Though there have been notable advancements, the field of secondary flow injection in C-D nozzles still has its share of challenges. Since experimental researches, CFD analysis, and hybrid analysis utilize different geometrical configuration of nozzles, injectors, boundary conditions, turbulence models, and performance measures, it becomes impossible to draw any meaningful comparisons. While some researchers prefer thrust vector angle, others prefer thrust coefficient, discharge coefficient, vectoring efficiency or pressure recovery ratio. Hence, the research field does not have a consistent methodology where a coherent link between different flow phenomena and design implications could be established. Moreover, most of the studies tend to examine a limited range of parameters or only a particular nozzle geometry instead of identifying generalized parametric trends based on the variations in injection location, angle, and pressure ratio. Validated scaling laws for planar, axisymmetric and serpentine geometries which would correlate shock topologies and separation characteristics to vectoring efficiency are also few[14].

These deficiencies lead to an obvious research gap: the lack of a comprehensive and design-based analysis of secondary flow injection for fluidic thrust vectoring in converging-diverging nozzles. The importance of this problem lies in the necessity of achieving a high level of vectoring capability with minimum penalty in terms of the amount of thrust loss, low flow consumption, and stable performance of the inner nozzle. In the absence of a coherent analysis of the existing literature, it is still challenging to determine the key design parameters, their interconnection, and the conditions to focus on. Hence, the need arises for an analysis of existing literature with respect to key physics involved, parameter influence, computational techniques, and outstanding problems.

Thus, the goal of the current review is to offer a systematic and thematic overview of the scientific work done to investigate secondary flow injection in convergent-divergent nozzles applied in fluidic thrust vectoring systems. Specifically, the review will attempt to cover the underlying flow physics, the comparison of effects of different geometric and aerodynamic parameters, the description of various computational and experimental techniques used to analyze such systems, and the discussion of key open questions in the field. Moreover, an additional goal of the review is to provide useful trends that could serve as guidelines for

designing such nozzles in the future, especially when high vectoring angles have to be attained at low losses in thrust and minimal secondary flow consumption.

The focus of the paper is restricted to flow-induced thrust vectoring in converging-diverging nozzles and their derivatives based on the control of internal compressible flows. Other thrust-vectoring techniques, mechanical in nature, are referenced for comparative purposes and do not form the core of the subject of investigation. The review highlights the effect of the location of secondary flow injection, its angle, the ratio of pressures, mass flow ratio, divergence of the nozzle, and separation of flows. The intention of such a review is to relate the physics of shock wave and boundary layer separation formation with the engineering aspects of control authority and thrust efficiency. It begins with an introduction to the flow physics and parameters followed by the review of the trends observed in the literature and finally the challenges associated with the subject.

2. Methodology

This is a systematic review based on PRISMA 2020 criteria regarding the effects of secondary flow injection in converging-diverging (CD) nozzles in fluidic thrust vectoring (FTV). The methodology guarantees that the process of literature selection and analysis, which consists of 30 papers published between 2019 and 2024, is transparent and reproducible, and will focus on CFD simulations, nozzle performance, and vectoring effectiveness.

This is a systematic review with qualitative synthesis mapping the secondary injection mechanisms (such as shock vector control, Coanda effect) in CD nozzles for FTV. Meta-analysis has not been conducted owing to heterogeneity in CFD and experimentally obtained results. The fundamental question of this systematic review is: how does secondary flow injection affect thrust vector angle, side force, and flow separation in CD nozzles for FTV? Supersonic/hypersonic regimes and NPR >4 are stressed in literature. Searches were conducted using Scopus, Web of Science, Google Scholar, and AIAA databases from 2000 to 2024. Key phrases searched for included "Secondary Flow Injection," "Fluidic Thrust Vectoring," "CD Nozzle," "Shock Vector Control," "Coanda FTV," and "Bypass Dual Throat Nozzle" in conjunction with boolean operators. Search results: ~100 total; duplicates excluded: 50, Most Related: 25. Study type: Peer-reviewed articles/conference papers on CFD/experimental FTV in CD nozzles.

- Relevance: Secondary injection for vectoring (e.g., bypass DTN, SVC); supersonic flow; quantitative metrics (vector angle, Cd, Cf).
- Language: English.
- Exclusions: Mechanical TVC, non-CD nozzles, subsonic-only, non-peer-reviewed.

Mechanism	Key Parameters	Vector Angle (°)	Cf	Cd	Studies
Bypass DTN	We=3.7mm, NPR=4	20.98	0.944	0.983	Wang 2019
SVC	Injection at throat	Up to 25	0.957	-	Multiple

Coanda	Parallel injection	22	-	-	Deng 2014

Database bias (e.g., Scopus emphasis on CFD); limited hypersonic experiments; no meta-analysis due to variability. Future: Include patents, expand to 2026+

3. Literature Review

The use of fluidic thrust vectoring (FTV) technology has become feasible due to the reduction in structural complexity and number of moving parts, as well as possible increased speed of the response in harsh thermomechanical conditions, when compared to traditional thrust vectoring technologies such as gimbaling nozzles, jet vanes, and flaps. For secondary injection type FTV systems, the mass flow rate of a high-pressure secondary stream is injected into a convergent-divergent (C-D) nozzle at a properly chosen axial station and angle. Secondary fluid mixes with the core supersonic flow and creates an asymmetric pressure pattern in the nozzle wall that produces the deflection of the resultant thrust vector. In other words, the effect of control action is created as a result of a strong coupling between jet momentum, shock wave structure, boundary layer separation, recirculation, and reattachment. The operation of these systems depends on various nondimensional parameters such as nozzle pressure ratio (NPR), secondary to primary pressure ratio (SPR), secondary to primary mass flow ratio, injector position and angle, and geometric parameters of the divergent part. NPR determines the general expansion conditions and creation of shocks and separation inside the system. The strength and penetration of the secondary jet with respect to the main one depend on the values of SPR and mass flow ratio. Injection location is especially important due to the dependence of the Mach number, static pressure, and boundary layer thickness on the position in the nozzle. Therefore, injection near the areas of higher Mach number and lower pressure results in greater asymmetry and vectoring effect. The injection angle has impact on jet penetration and mixing, although the main influence is defined by the combination of position and pressure ratio. Thermodynamic characteristics of the injected gas (molecular weight, temperature) define the effective density and momentum ratios.

3.1 Dual-throat and bypass dual-throat nozzles

The dual throat nozzles (DTN) take advantage of the recessed cavity created between two geometric throats to achieve controlled separation and reattachment of the supersonic core, thus resulting in a deflected jet without any solid components movement. Wang et al. have proposed the axisymmetric divergent bypass dual throat nozzle (ADBDTN), where a bypass channel along the circumference of the nozzle provides flow to the cavity and changes the separation topology while the main jet expands through two different throats. It is reported by the authors through their RANS calculations that the thrust vectoring process of the nozzle is still separation-based, where the main jet is vectored by an asymmetric separation region in the cavity. However, the bypass flow causes the shift of cavity pressure and separation region that enables large pitch vector angles to be achieved at a minimal loss in thrust coefficient. A maximum pitch vector angle of approximately 20.98° for a case with the following parameters can be achieved with

thrust and discharge coefficients of approximately 0.944 and 0.983 respectively for NPR = 4. Expansion ratio 1.2, bypass width 3.7 mm, throat rounding radius 8 mm, and cavity bottom radius 10 mm.

Continuing along this line of reasoning, Huang et al. performed a systematic parametric study of a planar bypass dual throat nozzle (BDTN) to determine the effect of bypass geometry and valve motion characteristics on vectoring performance. Utilizing a CFD configuration proven through comparison with experimental data (density based solver, realizable k–ε model, standard wall functions and Sutherland viscosity), they systematically varied bypass radius, valve axial location, and valve opening direction for low secondary mass flow ratios representative of actual configurations. According to their findings, the effect of bypass radius on vectoring angle is relatively insignificant in this case, while the effect of valve position and opening direction on the deflection angle, coefficient of thrust and flow field stability inside the nozzle is highly pronounced. More importantly, a completely open bypass does not result in maximal vector angle in all cases; rather, the most effective vectoring is obtained for particular bypass openings that correspond to maximal secondary jet total pressure, velocity, and injection angle of the bypass. In cited experimental researches, maximal vector angles up to 32° are observed for optimally designed BDTN at appropriate NPR.

3.2 Dual-bell nozzles and fluidic control of transition

Altitude compensating nozzle designs such as the dual bell nozzle consist of a low expansion “base” nozzle and a high expansion “extension” nozzle which are divided by a contour inflection point fixing the sea level separation point. The flow separation in the dual bell nozzle occurs at the inflection point at low NPR and hence mimics a low expansion nozzle while at higher NPR separation front moves downstream and hence the nozzle operates in altitude mode with improved vacuum performance. Studies carried out both experimentally and numerically have established that transition in such designs is hysteretic and non axisymmetric and can lead to substantial side forces, especially during the start of transition and re-transition process. Zmijanović et al. quantified the transition regimes for an axisymmetric dual bell nozzle and showed that the transition occurs at NPR lower than the theoretical one and is dependent on the shape of inflection point and wall pressure gradient in the extension region. Stark et al. developed a cooled film dual bell nozzle for a LOX/GH_2 thrust chamber and performed extensive RANS calculations to achieve homogeneous hot gas distribution and hydrogen film formation prior to hot fire testing. The computational study revealed the nominal NPR for mode transition around 80 in the baseline configuration and proved that not only cooling film mass flow but also mixture ratio (ROF) could be considered as fluidic “control knobs” for the mode transition advancement or delay. Thus, an increase in the hydrogen film mass flow by 50 g/s caused the earlier mode transition ($NPR_{trans} \approx 78.5$) and the decrease in film flow led to later transition ($NPR_{trans} \approx 81.5$). Similarly, an increase in ROF from 6 to 7 resulted in the early mode transition at NPR ≈ 77.5 and a decrease in ROF to 5 caused late transition to NPR ≈ 83.5. Moreover, Verma et al. also found that the location of injection of the secondary film cooling

flow is also an important factor affecting the separation location and wall temperature field; when the main flow is 2842 K and the coolant is 500 K, it can be seen that injecting at the inflection point location is much better than the throat and base nozzle locations because the value of separation location changes to $\zeta_{sep} = 6.12$ for NPR = 40 and Mach 2 secondary, while it was $\zeta_{sep} = 5.0\text{-}5.2$ otherwise. More recent studies by Benadda et al. used radial secondary injection following the inflection for active control of dual bell transition and side loading. They demonstrated that the mass flow ratios in transversal secondary flow of roughly 4–7.7% of primary flow are necessary in order to effectively change the time of transition. But since the injection of the secondary flow always leads to decrease in nozzle thrust coefficient, this technique should be used carefully in the case of propellant constrained launches. Overall, these studies proved that it is possible to use dual bell nozzles together with fluidic techniques such as secondary flow injection, film cooling, and mixture ratio manipulation to control transition and side loading with relatively low secondary flow ratios.

3.3 Shock-vector control in serpentine nozzles

The Serpentine nozzles having S-shaped inner passage are interesting for next generation fighter jets since they protect the turbine blades from being visible through direct line of sight and have lower signatures in terms of both infrared and radar. The curved shape causes large transverse pressure gradients, streamwise vortices and non-uniformity of exit profiles, making difficult the application of Shock Vector Control (SVC) methods for the cases of axisymmetric and planar nozzles. Recently, Hui et al. proposed a “high efficiency shock vectoring control serpentine nozzle” (SVCSN), which uses not only the main secondary injection passage but also auxiliary passage, thus providing a possibility to apply the method of Thrust Vectoring and at the same time improve the IR stealth performance. Using schlieren visualization, wall pressure measurements and RANS simulations, they performed the comparative analysis between conventional and high efficiency SVCSN and investigated the influence of NPR, SPR, secondary flow area As, and angle θ. The authors demonstrate that the injection of an auxiliary jet increases the distance between the legs of the lambda-shaped shock formed due to the injection of the secondary jet, which results in the expansion of the separation region and high-pressure region on the bottom wall downstream. The increase in the thrust vectoring angle and efficiency is thus obtained. For NPR = 6, the proposed high-efficiency SVCSN can provide the thrust vector angle and efficiency that are 61.6% and 75.7% higher than those obtained for conventional SVCSN. Moreover, NPR and SPR were demonstrated to have strong coupling effect on vectoring performance such that larger NPR together with smaller SPR produce better vectoring, with the NPR–SPR fluctuations of the vector angle and efficiency being about 22% and 64%, respectively. The vectoring efficiency was demonstrated to decrease monotonously with increasing relative secondary flow area, and smaller injection angles are recommended. Normal injection of 90° produces about 20% larger vector angle and efficiency than inclined injection of 110° for NPR = 6. Based on this data, the authors propose secondary flow area ratio $As \approx 0.06$ and injection angle $\theta \approx 90°$ as a good combination for high efficiency SVCSN.

3.4 Secondary-injection configurations and fuel effects

In the traditional secondary injection thrust vector control (SITVC) system of rocket nozzles, there is only one injector which exists in the divergent part at the station where the flow is supersonic, resulting in strong bow shock, separation region and pressure redistribution creating the side force by injecting a jet from that port. But it has been observed that splitting the flow from the secondary port into multiple ports and spacing them appropriately helps improving the vectoring capability and stability of flow for a certain value of the total mass flow of the secondary flow. The simulations of dual ports SITVC conducted by Mohammadi and Toloei using 3-D RANS revealed that positioning the first port in the optimal axial position ($x/Dt \geq 1$ down stream of throat) and the second port at least 8.5 injector diameters downstream of the first port creates higher side force and reduces the effect of bow shock impingement on the other side wall than a single port injector of the same total secondary mass flow. In another study, Sharma et al. have applied the same principle to a double secondary injection system in a 2D supersonic nozzle, where ANSYS Fluent has been used for comparing a single injection point situated at 10 cm distance downstream of the throat, with various dual injection arrangements for different inter port distances. In this study, when the inlet pressures for the primary and secondary injection were 5-7 MPa and 3-5 MPa respectively, then it was observed that for an inter-port distance of 3 cm between the fixed and movable ports, the thrust generation capability for the double injection system was around 299.6 kN as compared to the single injection system which had a value of 250.2 kN. In addition to that, the exit Mach number rose from 4.4 in the case of the single port system to about 4.9 in the case of the double port system. Also, the flow field inside was stable and shock impingement on the nozzle wall surfaces was unlikely. A mixed fluidic control approach was suggested by Ali et al., where TSTM is achieved by secondary fluid injection close to the throat and SVC is accomplished by fluid injection in the divergent part of a 2 D C-D nozzle. Design of Experiments showed that for TSTM case, better performance is obtained with smaller injector size and larger injector angle along with higher injection pressure, while optimal results for SVC case are obtained when the induced oblique shock just hits the opposite wall of the nozzle. If both TSTM and SVC are combined, the throat modulation capability is somewhat lost due to additional mass flow in SVC, but it is possible to have the same vector angle with reduced mass flow of SVC when compared to SVC alone. Almost all SITVC and DTN works assume the use of inert injectants; however, Salimi et al. studied fuel reacting dual throat nozzles where 3-D compressible reacting flow simulation of methane as well as other fuels injecting from slots or circular port was conducted. With NPR equal to 4, slot injection of methane with secondary to primary mass flow ratio equal to 9% generated a maximal thrust vector angle of around 17.1o and had relatively larger discharge coefficient, vector angle and vectoring efficiency than circular injection under same conditions. At lower secondary mass flow ratio of 2%, slot injection resulted in around 8% larger vector angle and 34% larger vectoring efficiency than circular injection. It was observed that lighter fuels (having low molecular weight) showed relatively better performance in terms of thrust ratio, vector angle and vectoring efficiency while heavy fuels provided slightly higher discharge coefficient.

Increase in center-to-center spacing between circular injector holes had increased thrust ratio but reduced discharge coefficient, vector angle and vectoring efficiency.

3.5 Passive internal-flow control and thermal-management flows

Although active secondary injection remains the core concept of fluidic thrust vectoring, there exist passive geometric changes that can have great effects on internal pressure distribution, base drag, and mixing and might be used together with secondary injection in order to obtain better results. In their study devoted to base pressure management in suddenly expanded duct with the C–D nozzle before it, Sethuraman et al. investigated the effect of inserting several rib of rectangular cross-sections of various heights in a square duct. They found out that at Mach 1 flow rib leads to decrease of base pressure and is good for applications where mixing is important for combustion. But at supersonic flow Mach number and at expanded flow condition, ribs are able to lead to substantial increase in base pressure in recirculation zone. In particular, at $M = 1.64$ and $NPR \approx 7$ a rib with height to duct height ratio $h/H = 0.23$ located at $x/H = 2.75$ resulted in increase of base pressure by about 58% comparing with the ribless case. For applications in turbomachines, Chen et al. considered the effect of endwall cooling and aerodynamic performance on a nozzle guide vane passage equipped with a 2D contoured hub and a leakage slot located upstream. With 3D RANS analysis using SST γ–θ transition model, they investigated 16 different mass flow ratio (MFR) levels for slot leakage from 0.125% to 2% of the main flow and revealed that there is an optimal range of MFR in terms of providing maximum adiabatic effectiveness and minimum total pressure loss coefficient, because too small MFR will induce hot gas ingestion and too large MFR will increase the aerodynamic losses. The results indicated that the use of endwall contouring accelerated and thinned the boundary layer and weakened secondary vortices so that it provided reduction in the aerodynamic loss and better coolant coverage compared with the flat wall condition. The same phenomena have been observed for film cooling of dual bell and spiked blunt body, where secondary coolant jets not only provide thermal protection but also affect separation/recirculation regions.

3.6 Real-fluid and multiphase considerations

A number of more recent investigations point to the importance of real fluid thermodynamic effects and multiphase physics on the nozzle internal flow field and, consequently, on fluidic thrust vectoring effectiveness. Raman and Kim modeled the flow of supercritical CO_2 through C-D nozzles employing different equations of state (EOS) and demonstrated a high sensitivity of the shock strength, shock position, and temperature jump across the normal shock to the choice of EOS at the vicinity of the critical point. Lyras et al. modeled LOx flow in C-D nozzles for both subcritical and supercritical outlet conditions and found that in the subcritical case the flow is supersonic, exhibits shock trains, and experiences strong cooling while in the supercritical one the flow is smooth and subsonic and decelerating with no shock waves. In classic studies conducted by Ranger and Nicholls with respect to aerodynamic fragmentation of water drops after shock passage in air (shocks Mach number of 1.5-3.5 and droplet sizes of 750-4000 μm), it

has been found that the breakup process under the high Weber numbers depends mainly on the dynamic pressure and drop size due to the existence of boundary layer stripping phenomenon. The analysis and measurement of their breakup time reveal that in usual conditions of nozzles operating at high speeds, there is the possibility of fragmentation and rapid vaporization of sufficiently small fuel drops so that the flow can be considered gaseous during its interaction with core shocks and separation regions, provided favorable values of Weber numbers and residence times. Despite all the above, the collective experience from S CO_2, LOx, and two-phase research demonstrates the necessity of considering appropriate real fluid equations of state, cavitation and spray breakup correlations while designing the fluidic thrust vectoring system.

Ref	Nozzle/ Configuration	Mechanism / Concept	Key Operating Parameters	Main Quantitative Findings
[6]	Axisymmetric divergent bypass dual-throat nozzle	Separation in recessed cavity; bypass modifies cavity pressure and separation topology	ER≈1.2; bypass width≈3.7 mm; throat r≈8 mm; cavity r≈10 mm; NPR=2–16	At NPR=4, δ≈20.98°, Cf≈0.944, Cd≈0.983 (vectored); Cd≈0.983 non-vectored across NPR 2–16
[11]	Planar bypass dual-throat nozzle	Bypass channel feeds cavity; adaptive valve controls secondary jet	NPR≈4; small secondary fraction; varying bypass radius, valve position and opening direction	Bypass radius minor effect; valve position/direction strongly affect δ and Cf; max δ≈32° for optimized settings
[15]	Dual-bell nozzle with inflection and film / secondary injection	Altitude-compensating dual-bell; separation at inflection; film and secondary flows tune transition and side loads	Transition NPR≈78–83 depending on film mass flow and ROF; NPR up to ≈100	Transition hysteresis with side loads; film mass flow and ROF shift NPR_trans by several units; radial injection effective only above ~4–7.7% secondary mass, with Cf penalty
[16]	Dual-bell with radial secondary injection in extension	Radial secondary jet at inflection to delay/advance regime transition	Secondary mass ratio≈4–7.7% of primary; NPR sweep across transition	Secondary injection delays transition and reduces side loads, but reduces base-nozzle Cf; chamber/slot geometry also influences transition
[17]	Shock-vectoring serpentine nozzle with auxiliary duct	Main and auxiliary secondary jets create λ-shock and asymmetric separation in serpentine duct	NPR=6; varying SPR; As; θ=90–110°	High-efficiency SVCSN: δ and VE ≈61.6% and 75.7% higher than conventional; best at As≈0.06 and θ=90°; larger NPR with smaller SPR improves performance
[18]	C–D nozzle with two side-injection ports	Two secondary jets in separated regime to enhance side force and avoid bow-shock impingement	First port at optimized x/Dt; second port ≥8.5 port diameters downstream; NPR≈4	Dual-port configuration yields higher side force and better vectoring than single port at same total secondary mass; reduces opposite-wall shock impingement
[12]	2-D supersonic nozzle with single vs dual fuel injectors	Dual secondary fuel ports in divergent section for SITVC	Primary inlet 5–7 MPa; secondary 3–5 MPa; first port 10 cm from throat; second port Δx=0–4 cm	At Δx=3 cm, thrust≈299.6 kN vs 250.2 kN (single); exit M≈4.9 vs 4.4; dual system more stable with less shock impingement
[19]	2-D C–D nozzle with throat-shifting and SVC jets	Combined thrust modulation near throat and SVC in divergent section	DOE over injector area, angle, pressure; NPR, SPR varied	Optimal TSTM uses small area/angle, high pressure; SVC optimal when induced shock just reaches opposite wall; combining TSTM+SVC cuts SVC mass flow for given δ but reduces modulation efficiency
[20]	Planar dual-throat nozzle with fuel (slot/circular)	Combustion-assisted DTN vectoring; reacting secondary jets in cavity	NPR=4; secondary mass 2–9% of primary; slot/circular injectors; multiple fuels	Slot methane at 9% gives δ≈17.1°; at 2% secondary, slot δ≈8% and VE≈34% higher than circular; light fuels yield higher δ,

	injection			VE, and thrust ratio; heavy fuels slightly higher Cd; larger spacing improves thrust ratio but reduces δ, VE, Cd
[14]	C–D nozzle into square duct with rectangular ribs	Passive base-pressure control with ribs in suddenly expanded duct	M=1,1.36,1.64,2; NPR=1.5–10; h/H=0.10–0.23; x/H≈0.283–2.75	At M=1.64, NPR≈7, h/H=0.23 at x/H=2.75 increases base pressure ≈58%; recommended rib height≈4–6 mm at 4–5H
[21]	2-D contoured endwall NGV with upstream slot leakage	Slot leakage for endwall cooling; contouring reduces secondary-flow loss	MFR=0.125–2% of mainstream; slot at 0.25 C_ax upstream	Intermediate MFR band gives high cooling effectiveness with low loss; low MFR causes hot-gas ingestion; high MFR raises loss; contoured endwall weakens secondary vortices
[22]	C–D nozzles with S-CO2 and LOx flows	Real-gas EOS and phase effects on shocks and separation	Near-critical S-CO2; LOx sub- and supercritical outlets	EOS choice shifts shock location and temperature rise; subcritical LOx has shock trains and strong cooling; supercritical case smooth, subsonic deceleration; affects FTV behavior in cryogenic regimes
[23]	Water drops behind shock waves in air	Shock-induced aerodynamic shattering (boundary-layer stripping)	Shock Ms=1.5–3.5; D=750–4000 μm; high Weber	Breakup governed mainly by dynamic pressure and drop size; supports rapid atomization and gaseous-behavior assumption for fine sprays in SITVC/DTN regions

4. Results and Discussion

4.1 Vectoring authority and secondary-flow economy

For dual throat, bypass dual throat, serpentine SVC, and fuel reacting dual throat nozzles, it is found that considerable vector thrust angles can be obtained through moderate secondary flows and without many sacrifices in terms of discharge coefficient, if the nozzle geometry and secondary injection are co-design considerations. For ADBDTN, it is revealed by Wang et al. that the flow adaptive design for NPR = 4 has a pitch vector angle of 20.98° with a thrust coefficient of 0.944 and a discharge coefficient of 0.983 when it is vectored and with Cd ≈ 0.983 in the case that it is not vectored at NPR 2 - 16, which indicates that the mass flow performance of this nozzle is near the ideal value. In BDTN, Huang et al. obtain vector thrust angles as large as 32° for particular configurations of bypass valves at moderate NPRs, along with small secondary mass flow ratios. For SVC using serpentine configuration, Hui et al. show that the addition of a separate duct for making a high-efficiency SVCSN leads to a rise in the thrust vector angle and vectoring efficiency by 61.6% and 75.7%, respectively, for NPR = 6 as compared to a regular SVCSN, besides being able to use less secondary flow owing to better coupling of shock separation. For fuel reacting DTNs, Salimi et al. reveal that the injection of methane via slots at a secondary to primary mass flow ratio of 9% produces a maximum thrust vector angle of 17.1°, besides slot injectors outperforming the circular injectors regarding discharge coefficient, vector angle, and vectoring efficiency. With even 2% secondary mass flow, the slot injectors offer 8% more vector angle and 34% more vectoring efficiency than circular injectors. SITVC investigations with multi-port configurations validate the fact that redistribution of the total mass flow from secondary inlets in multiple ports helps improve the vectoring capability and flow stability. Mohammadi and Toloei prove that placement of a second

port at a distance of at least 8.5 times the port diameter after optimization of the first port leads to an increase in side force and decrease of shock impingement on the body of the nozzle compared to a single port setup. Sharma et al. observe that in case of dual secondary injection with 3 cm distance between two ports, the thrust is 299.6 kN and exit Mach number is ≈4.9 in contrast with the single injection where thrust and Mach number are 250.2 kN and ≈4.4 correspondingly, at the same inlet pressure of 5–7 MPa and secondary pressure of 3–5 MPa. It is clear from the above discussion that flow turn vectoring technique needs optimum design of the geometry and injectors.

4.2 Complementary roles of geometry and fluidic control

It is clear from the literature review that both geometry shape and fluidics contribute complementarily in deciding the process of separation, the authority of vectoring and side loads. Geometric elements like cavities, dual throats, contour inflections, dual divergences, and serpentines precondition the supersonic flow, which sets the pattern of shocks and separations. For instance, the dual divergent planar nozzle developed by Nair et al. does not produce an asymmetric separation region and decreases the side loads during over-expanded conditions only by varying the Mach number of inner nozzle geometry and its length without using any secondary flow. Similarly, dual throat and dual bell geometry provide controlled separation regions either in cavities or inflection that can be utilized even by little secondary/coolant flow. Secondary injection is used then merely to bias or correct these existing structures so as to attain the required vector angle, transition dynamics, or thermal loading pattern. In ADBDTN and BDTN, bypass flows are used to control the cavity pressure and separation pattern such that large vector angles can be attained without substantial loss of mass flow. In dual bell nozzles, film cooling flows and mixture ratio change cause an NPR shift of a few numbers and separation displacement to control side loads without changing the nozzle geometry. The combination approach of Ali et al. TSTM + SVC proves that throat shifting injection is capable of controlling effective area and thrust whereas SVC injection provides vectoring; their combination results in lowering the required mass flow of the SVC injection for achieving certain vector angle but lowers the modulation efficiency because of the interaction effects at the throat. The multiport SITVC experiments have demonstrated that by using secondary injection at multiple ports with appropriate spacing, better vectoring capability and lower shock impingement resulting side loads can be achieved compared to a single port arrangement.

4.3 Side-load management and start-up behavior

Side loads on start up, transition, and re-transition continue to be a problem for high area ratio nozzles and engine clusters, and various papers discuss the reduction of side loads using fluidic and geometry-based strategies. Zmijanović et al. and subsequent experiments have shown that transition from sea level to altitude mode in dual bell nozzles takes place within an NPR range that is non-axisymmetric in nature, thus creating side loads which may amount to several percent of axial thrust without proper control. Benadda et al. have found that radial secondary injection

near the inflection point causes the transition to take place either earlier or later and thus allows delaying the onset of side loads; however, this is possible only when secondary mass flow fractions are larger than 4–7.7%, but results in lower base section thrust coefficient. In contrast, Stark et al. and Verma et al. prove that small changes in coolant film mass flow and Mach number are sufficient to change the NPR of transition and separate the shock, without any significant penalty in thrust. Sreerag et al. have considered the problem of side load alleviation through use of an annular jet injection into bell nozzles along the nozzle lip with flow direction being parallel to or at an angle to the main flow. Their studies showed that for certain values of secondary NPR a parallel annular jet is able to postpone or even suppress internal separation under overexpanded regime at relatively low chamber pressures, thus, preventing the occurrence of shock-induced separation responsible for the generation of startup side loads. Inclined injection (with ±5°–10° inclination angles) is not as efficient and requires higher secondary pressure. Rib geometries in a suddenly expanded duct (studied by Sethuraman et al.) also impact base pressure and therefore the base-induced side loads; in particular, with M = 1.64 and NPR = 7 and h/H = 0.23 at x/H = 2.75 base pressure increased by 58% which can be used to design specific pressure distributions on the afterbody surface.

Numerical performance characteristics of the 2-D supersonic convergent-divergent (CD) nozzle for varying SITVC nozzle designs are shown in Figure 1 below. There exists an observable, coupled correlation between secondary injection port spacing and thrust produced by the nozzle, as well as exit Mach number. In case of the dual-port designs, the port spacing affects the nozzle performance significantly. The Dual (4 cm) nozzle design has the lowest performance metrics among all the cases considered in the current study, generating thrust of 100.5 N and exit Mach number of 2.79. But, the reduction in port spacing leads to improvement in the performance. The Dual (3 cm) nozzle design shows improved performance as compared to the basic Single Port case. The Dual (3 cm) nozzle generates the best performance metrics possible in the current study setup, producing maximum thrust of 299.6 N and the highest exit Mach number of 4.90. These results indicate that the optimal multiple port secondary injection spacing can effectively prevent undesirable secondary shocks and flow separation effects[12].

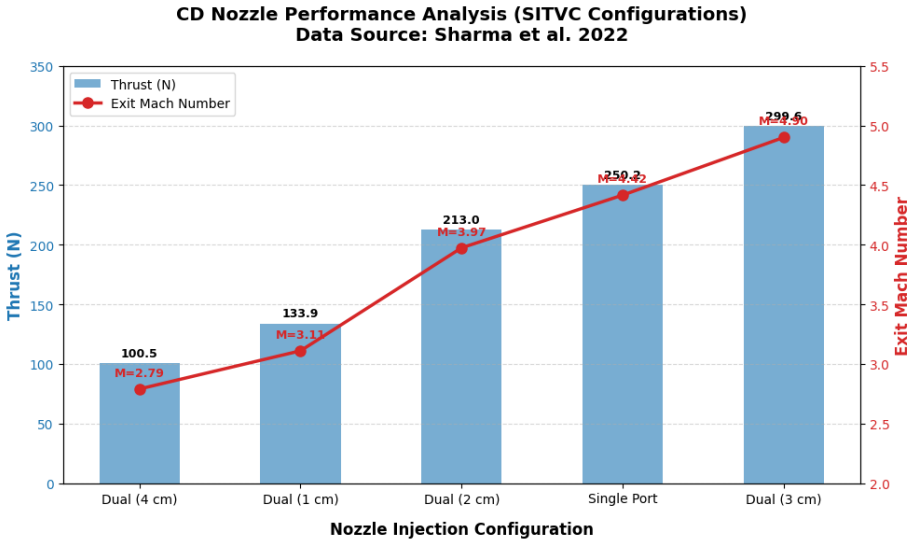

Figure 1: Performance comparison of a 2-D supersonic convergent-divergent (CD) nozzle under various secondary injection thrust vector control (SITVC) configurations.

4.4 Real-fluid and thermal-management constraints

In the case where FTV is implemented in the cryogenic or high pressure transcritical conditions, the real properties of the fluid and considerations of heat removal create further design constraints for the nozzles. In S CO_2 and LOx nozzle studies, it has been found that selection of the equation of state and the condition, whether it is subcritical or supercritical, greatly affects the shock position, temperature increase, and entropy generation; hence, separation points and FTV characteristics will be different from those of the gas flow modeled through an ideal gas equation of state. LOx simulations carried out by Lyras et al. have shown that subcritical state creates shock trains and significant cooling effects like in gas nozzles, while supercritical condition results in gradual deceleration without any shocks. It should be clear that thermal management flows like film cooling and endwall leakage need to be properly designed for achieving thermal and aerodynamic targets, as evident from NGV and dual bell analyses where slight variation in coolant mass flow ratio causes major influence on cooling performance, total pressure drop, and separation characteristics. Lastly, phase change and droplet shattering research clearly shows that in the case of high Weber numbers prevailing in rocket exhaust and hypersonic applications, sufficiently fine spray will always shatter and vaporize quickly; hence, there is justification of gaseous assumption in many SITVC/DTN formulations. In summary, the outcomes discussed above have indicated that for achieving the high levels of performance and sustainability in fluidic thrust vectoring, a holistic methodology is required to take into account the issues related to geometry design, secondary injection arrangement, mass flow and momentum budgets, real fluids thermodynamics, and thermal flows, among other factors.

References

[1] V. Yadav and P. K. Tiwari, “A Review on CFD Analysis of Effects of Convergence and Divergence Angles on the Performance of a Nozzle,” *Int. J. Sci. Res. Eng. Trends*, vol. 6, no. 1, pp. 33–35, 2020, [Online]. Available: https://ijsret.com/wp-content/uploads/2020/01/IJSRET_V6_issue1_108.pdf

[2] A. F.EL-SAYED, *AIRCRAFT PROPULSION AND GAD TURBINE ENGINES*.

[3] J. Anderson, *Fundamentals of Aerodynamics*. 2019. doi: 10.1002/9781119500377.ch4.

[4] G. P. SUTTON and O. BIBLARZ, *ROCKET PROPULSION ELEMENTS*.

[5] J. D. Mattingly and K. M. Boyer, *Elements of Propulsion: Gas Turbines and Rockets Second Edition*. 2016. doi: 10.2514/5.9781624103711.0000.0000.

[6] Y. Wang, J. Xu, S. Huang, Y. Lin, and J. Jiang, “Computational study of axisymmetric divergent bypass dual throat nozzle,” *Aerosp. Sci. Technol.*, vol. 86, pp. 177–190, 2019, doi: 10.1016/j.ast.2018.11.059.

[7] R. Stark, C. Génin, C. Mader, D. Maier, D. Schneider, and M. Wohlhüter, “Design of a film cooled dual-bell nozzle,” *Acta Astronaut.*, vol. 158, pp. 342–350, 2019, doi: 10.1016/j.actaastro.2018.05.056.

[8] Q. Qin and J. Xu, “Numerical evaluation of aerodome and cooling jet for aeroheating reduction,” *Aerosp. Sci. Technol.*, vol. 86, pp. 520–533, 2019, doi: 10.1016/j.ast.2019.01.046.

[9] L. Shi *et al.*, “Research progress on ejector mode of rocket-based combined-cycle engines,” *Prog. Aerosp. Sci.*, vol. 107, no. April, pp. 30–62, 2019, doi: 10.1016/j.paerosci.2019.03.003.

[10] V. Zmijanovic, L. Leger, M. Sellam, and A. Chpoun, “Assessment of transition regimes in a dual-bell nozzle and possibility of active fluidic control,” *Aerosp. Sci. Technol.*, vol. 82–83, no. February, pp. 1–8, 2018, doi: 10.1016/j.ast.2018.02.003.

[11] S. Huang, R. Pan, J. Xu, R. Gu, and Y. Zhang, “A parametric investigation of Dual-throat nozzle bypass channel configurations for advanced Aviation applications,” *Heliyon*, vol. 10, no. 18, p. e37752, 2024, doi: 10.1016/j.heliyon.2024.e37752.

[12] K. Sharma, P. M. S. S. Manohar, and A. K. Mishra, “Analysis and optimization of Dual secondary fuel injector for Thrust vector control,” *J. Phys. Conf. Ser.*, vol. 2272, no. 1, 2022, doi: 10.1088/1742-6596/2272/1/012002.

[13] Z. HUI, J. SHI, W. LIN, L. ZHOU, Z. WANG, and Y. LIU, “Experimental investigation and numerical analysis on high-efficiency shock vectoring control serpentine nozzles: Study on high-efficiency shock vectoring control serpentine nozzles,” *Chinese J. Aeronaut.*, vol. 37, no. 12, pp. 296–324, 2024, doi: 10.1016/j.cja.2024.09.013.

[14] V. Sethuraman, P. Rajendran, S. A. Khan, A. Aabid, and M. Baig, “Control of Nozzle

Flow Using Rectangular Ribs at Sonic and Supersonic Mach Numbers," *Fluid Dyn. Mater. Process.*, vol. 20, no. 8, pp. 1847–1866, 2024, doi: 10.32604/fdmp.2024.049441.

[15] L. Léger, V. Zmijanovic, M. Sellam, and A. Chpoun, "Experimental investigation of forced flow regime transition in a dual bell nozzle by secondary fluidic injection," *Int. J. Heat Fluid Flow*, vol. 89, no. March, 2021, doi: 10.1016/j.ijheatfluidflow.2021.108818.

[16] B. Sibanda, "Aerodynamic Analyses of Variable Geometry Asymmetric Supersonic Nozzles," no. 2007, 2020.

[17] V. Zmijanovic, L. Leger, E. Depussay, M. Sellam, A. Chpoun, and E. Numerical, "Experimental – Numerical Parametric Investigation of a Rocket Nozzle Secondary Injection Thrust Vectoring To cite this version : HAL Id : hal-02398152 Experimental – Numerical Parametric Investigation of a Rocket," pp. 0–18, 2021.

[18] E. Mohammadi and A. Toloei, "Analysis of dual secondary injection for thrust vectoring," *Aircr. Eng. Aerosp. Technol.*, vol. 83, no. 4, pp. 213–220, 2011, doi: 10.1108/00022661111138620.

[19] A. Ali, C. G. Rodriguez, A. J. Neely, and J. Young, "Combination of fluidic thrust modulation and vectoring in a 2D nozzle," *48th AIAA/ASME/SAE/ASEE Jt. Propuls. Conf. Exhib. 2012*, no. August, pp. 1–13, 2012, doi: 10.2514/6.2012-3780.

[20] M. R. Salimi, R. Askari, and M. Hasani, "Computational Investigation of Effects of Side-Injection Geometry on Thrust-Vectoring Performance in a Fuel-Injected Dual Throat Nozzle," *J. Appl. Fluid Mech.*, vol. 15, no. 4, pp. 1137–1153, 2022, doi: 10.47176/jafm.15.04.33354.

[21] P. Chen, M. Alqefl, X. Li, J. Ren, H. Jiang, and T. Simon, "Cooling effectiveness and aerodynamic performance in a 2D-Contoured endwall passage with different mass flow ratios," *Int. J. Therm. Sci.*, vol. 142, no. May, pp. 233–246, 2019, doi: 10.1016/j.ijthermalsci.2019.04.031.

[22] S. K. Raman and H. D. Kim, "Solutions of supercritical CO2 flow through a convergent-divergent nozzle with real gas effects," *Int. J. Heat Mass Transf.*, vol. 116, pp. 127–135, 2018, doi: 10.1016/j.ijheatmasstransfer.2017.09.019.

[23] A. A. Ranger and J. A. Nicnolls, "Aerodynamic shattering of liquid drops," *AIAA J.*, vol. 7, no. 2, pp. 285–290, 1969, doi: 10.2514/3.5087.